Crystal structure of thioflavin-T and its binding to amyloid fibrils: insights at the molecular level†

Cristina Rodríguez-Rodríguez,[a] Albert Rimola,[b] Luis Rodríguez-Santiago,[a] Piero Ugliengo,[b] Ángel Álvarez-Larena,[c] Hugo Gutiérrez-de-Terán,[d] Mariona Sodupe*[a] and Pilar González-Duarte*[a]

Received (in Cambridge, UK) 26th June 2009, Accepted 2nd December 2009
First published as an Advance Article on the web 4th January 2010
DOI: 10.1039/b912396b

Combining X-ray data on thioflavin-T and theoretical calculations on its binding to a peptide model for $A\beta_{1-42}$ fibrils gives evidence of main stabilizing interactions, which influence the dihedral angle between the two moieties of thioflavin-T and thereby its fluorescence properties; these results shed new light on possible strategies for the design of dyes to bind amyloid fibrils more specifically.

The presence of amyloid fibrils is a key neuropathological feature in more than 20 diseases, including Alzheimer's disease (AD).[1] Most of these protein aggregates have a generic structure that consists of a continuous β-sheet.[2] The fluorescent dye thioflavin-T (ThT) has been commonly used to stain amyloid deposits in tissues[3] and to characterise the presence of amyloid fibrils.[4] Chemically, ThT is the chloride salt of a cation (ThT^+) that consists of an *N*-methylated benzothiazole fragment linked to a dimethylaniline ring (Fig. 1). The dihedral angle between these two planar moieties, ϕ, largely determines the spectral properties of this dye, as shown by Stsiapura *et al.*[5] from a computational study of the torsional relaxation of ThT^+ in the excited state. However, the mechanism of fluorescence enhancement upon ThT^+ binding to amyloid fibrils and the molecular understanding of this binding are still objects of intensive study.[6] Both issues are critical in order to design new dyes to bind amyloid fibrils more specifically,[7,8] and for the development of diagnostic and therapeutic agents.

Recently, we have shown that incorporation of chelating properties into well-known intercalation compounds such as ThT^+ may be a successful strategy for developing the next generation of agents for AD theragnosis.[9] Remarkably, there are no X-ray structural data on the free ThT^+ but only when bound to the *Torpedo californica* acetylcholinesterase (*Tc*AChE) protein,[10] one of the few examples showing that ThT^+ also binds to non-β-sheet cavities. Overall, in order to shed light onto ThT^+-binding interactions, we have undertaken an experimental and theoretical study of the structure of unbound ThT^+. Subsequently, we have examined its binding to the fibrillar core structure of $A\beta_{1-42}$ peptide[11] by combining docking and molecular dynamics (MD) strategies with quantum chemical calculations.

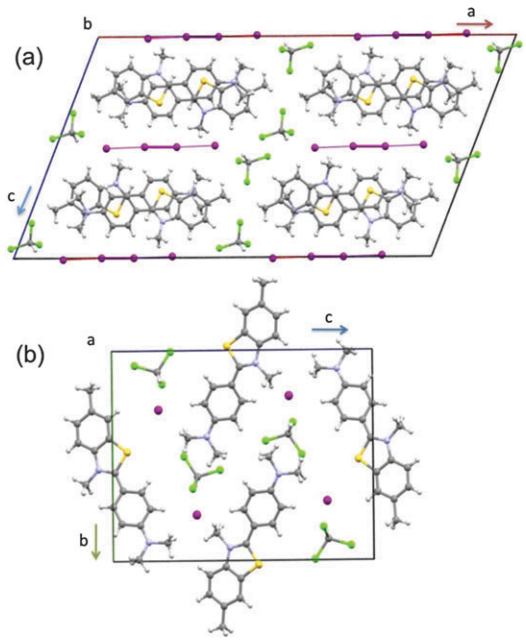

Fig. 1 Unit cells of **1** (a) and **2** (b): I_4^{2-} and I^- anions in purple; chlorine, nitrogen and sulfur atoms in green, blue and yellow, respectively.

Treatment of (ThT)Cl with NaI, as detailed in the experimental section (see ESI†), yielded X-ray quality crystals of $(ThT)_2I_4{\cdot}2CHCl_3$ (**1**) and $(ThT)I{\cdot}CHCl_3$ (**2**).[12] The unit cells are shown in Fig. 1. Both I_4^{2-} (**1**) and I^- (**2**) anions establish weak C–H···I interactions with the $CHCl_3$ solvent molecules. I_4^{2-}, whose formation is probably due to aerobic oxidation, shows a centrosymmetric essentially linear geometry, consistent with reported data.[13,14] This anion appears to be essential for the effective packing arrangement of the ThT^+ cations in **1**, which is formed in much shorter time than **2**. Our unsuccessful attempts to obtain any crystal structure under other experimental conditions evidence the relevance of the iodide anions and $CHCl_3$ solvent in the formation of X-ray quality crystals. Remarkably, the closest related analogs of ThT^+ with known crystal structures are not cationic species but neutral molecules.[15–17]

[a] *Departament de Química, Universitat Autònoma de Barcelona, 08193 Bellaterra, Barcelona, Spain. E-mail: mariona.sodupe@uab.cat, pilar.gonzalez.duarte@uab.cat*
[b] *Dipartimento di Chimica IFM and NIS Centre of Excellence, Università degli Studi di Torino, 10125 Torino, Italy*
[c] *Servei de Difracció de Raigs X, Universitat Autònoma de Barcelona, Barcelona, Spain*
[d] *Fundación Pública Galega de Medicina Xenómica, CHUS, 15786 Santiago de Compostela, Spain*

† Electronic supplementary information (ESI) available: Experimental, X-ray diffraction and computational details. CCDC 728298 and 728299. For ESI and crystallographic data in CIF or other electronic format see DOI: 10.1039/b912396b

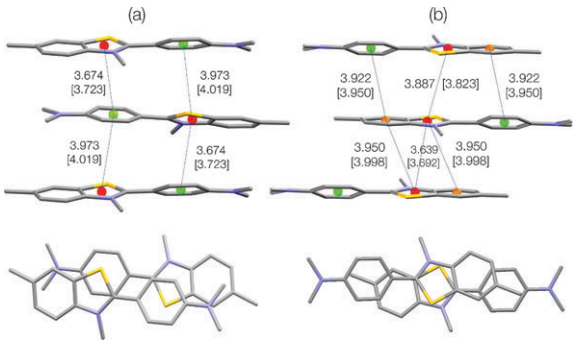

Fig. 2 Front and top view of the stacking arrangements in **1** (a) and **2** (b). X-Ray distances (in Å) between centroids are indicated by dashed lines. Periodic B3LYP values are in brackets.

The only crystallographically independent ThT^+ cation in **1** and **2** show very similar geometric parameters, the dihedral angle ϕ between the two planar benzothiazole and dimethylaniline moieties being 23.8(2)° in **1** and 20.0(2)° in **2**. In both crystal structures the ThT^+ cations are packed in columnar stacks, neighbouring cations having a head to tail disposition and their positive charge being on opposite sides to minimize Coulombic repulsion. Cations defining a stack in **1** are related by a twofold screw axis, while in **2** neighbouring cations are related by an inversion centre (Fig. 2). In both crystal structures the distances between stacked cations and their π–π facing reveals a trade-off between ring electric multipole and dispersion interactions. In **1** the main overlap is observed between thiazolyl and dimethylaniline rings (Th–Ph), whereas in **2** two different overlaps are present: a Th–Th interaction, and a partial Bz–Ph overlap (Bz denotes the benzene ring of benzothiazole).

The values of ϕ in **1** (24°) and **2**, (20°), are smaller than that previously computed for the isolated ThT^+ cation,[5] which ranges from 32° to 45°, depending on the adopted level of theory. This suggests that packing effects, particularly stacking interactions between ThT^+ cations in the crystal, are responsible for the decrease of this dihedral angle ϕ which, as mentioned, largely determines the spectral properties of this dye. To investigate this point, we have performed B3LYP calculations[18,19] of the ThT^+ cation either isolated or in crystals **1** and **2**. Periodic geometry optimizations were performed only for the internal atomic positions, the lattice parameters being frozen at the experimental values. This procedure has been shown to be a cost effective strategy for describing molecular crystals where dispersion forces are relevant[20] (see detailed discussion in ESI†) and it also holds for the present systems, since main optimized B3LYP parameters are in good agreement with the X-ray data, the computed distances differing by 0.05 Å at the most (Fig. 2). The ϕ value we have calculated for the isolated ThT^+ (35°) agrees with previously reported data[5] and is substantially larger than that we have obtained for **1** (20°) and **2** (19°). Noticeably, the latter values are consistent with those obtained from X-ray data, 24° (**1**) and 20° (**2**), which validates the reliability of our calculations and shows the importance of packing effects. Overall, the intrinsic ease of rotation around the C–C bond, which at the B3LYP level is computed to be 5 kcal mol^{-1}, and the relatively large stacking interactions in the crystals account for the increase in planarity of ThT^+ in the crystal structures. Within this context, a recent study on the X-ray structure of ThT^+ bound to *Tc*AChE[10] shows the ThT^+ ring system in a coplanar position packing parallel to aromatic residues. This packing causes a decrease in torsional relaxation of ThT^+ and, hence, an increase in its fluorescence.

Despite the wide use of ThT^+ as a fluorescent dye to determine the presence of amyloid fibrils, studies on the corresponding binding mode at the molecular level are scarce.[21,22] In order to make a further step, we have examined the interaction of ThT^+ with the fibrillar core structure of $A\beta_{1-42}$ peptide, as deduced from NMR data.[11] Thus, we have performed a series of automated docking, molecular dynamics and quantum mechanical calculations. The automated blind docking exploration involved 100 docking runs on each one of the ten protein conformers deposited under the PDB code 2BEG. In all 1000 solutions the ThT^+ cation was placed parallel to the long axis of the fibrils, in agreement with anisotropic fluorescence emission studies.[21] After clustering all docking possibilities, we identified six probable binding modes, which are located on four different binding sites, two within the inner core of the fibrils and the other two on the external surface (Fig. S1, ESI†). A deeper exploration of each binding mode by MD and binding free energy calculations, using the linear interaction energy approach[23] (see ESI for details†), shows that the two external binding sites, in which ThT^+ is accommodated into the crevices defined either by residues 33–35 (pose A) or 35–37 (pose B1), are the most favorable (Fig. 3). Remarkably, in both locations the planar dimethylamino moiety of ThT^+ is positioned nearly parallel to the main backbone of the polypeptide chain. The ease of rotation around the C–C bond of ThT^+ accounts for the orientation of the benzothiazole fragment, with the NMe^+ group pointing away from the crevice in pose A and towards the Met side chain in pose B1.

Among the two positions, pose B1 is more stable by 2.6 kcal mol^{-1} and encloses a ThT^+ cation with increased planarity (44°) if compared with unbound ThT^+ (65°) as simulated under the same conditions. This latter ϕ value resulting from the adopted OPLS force field is significantly higher than that calculated with B3LYP for ThT^+ in the gas phase (35°). Therefore, to keep coherence with the quantum mechanical method used, we have performed optimizations at the B3LYP-D level for ThT^+ interacting with a model of a β-sheet structure, made by five strands of the $CH_3(NHCOCH_2)_3NHCOCH_3$ peptide, which mimics the interaction with the polypeptide chain. Results confirm that

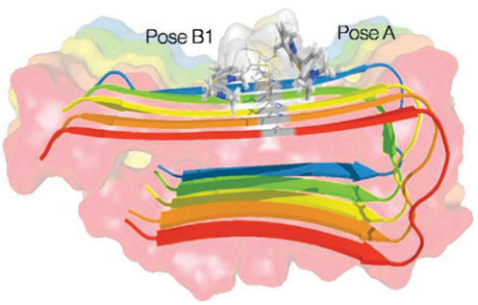

Fig. 3 External binding sites of ThT^+ bound to $A\beta_{1-42}$ from molecular dynamics calculations. ThT^+ is located in the crevices defined by the residues 33–35 (pose A) or 35–37 (pose B1).

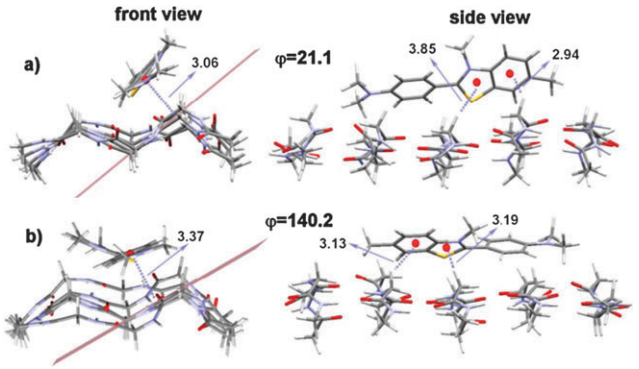

Fig. 4 B3LYP-D optimized structures of ThT^+ interacting with a model of the β-sheet structure. Distances are in Å. Front views show the distance between the centroid of dimethylaniline and the plane defined by the peptide bond atoms immediately below. Side views show the computed distances between the hydrogen of the Gly residue and the ring centroids of benzothiazole.

the dimethylaniline ring remains parallel to the peptide backbone, the distance between the centroid of the benzene ring and the mean plane defined by the atoms involved in the closest peptide bond being 3.06 Å (Fig. 4a). The concomitant decrease of ϕ down to 21° is mainly due to the stabilizing interaction between the benzothiazole fragment and the closest H(Gly), the distance between the centroid of the benzene ring and hydrogen being 2.94 Å. Overall, the minimum energy structure is mainly determined by π-stacking and weak CH–π interactions. Indeed, if dispersion forces are not taken into account in the calculation by adopting the plain B3LYP, the optimized structure shows that dimethylaniline is no longer parallel to the peptide bond, the distance between the centroid of benzene and the peptide bond plane increasing up to 4.0 Å and ϕ increasing to 32°. Moreover, we have located a second nearly degenerate energy minimum (0.2 kcal mol^{-1} below the previous one) with ϕ being approximately 140° (Fig. 4b). In this case, the dimethylaniline ring remains parallel to the peptide backbone and CH–π interactions are maintained with the nearest H(Gly) residue. Remarkably, the energy cost of internal rotation of ThT^+ bound to the fibril, estimated by performing a constrained geometry optimization with the dihedral angle of ThT^+ fixed at 90°, is 7 kcal mol^{-1}. This value, although somewhat larger than that obtained for unbound ThT^+ (5 kcal mol^{-1}) is not large enough to prevent internal rotation. These results suggest that interactions between benzothiazole and the side chains of the fibril are the ones responsible for the decrease of torsional relaxation in bound ThT^+.

In summary, the dihedral angle ϕ of ThT^+ in crystals **1** (24°) and **2** (20°) can be explained by considering π-stacking interactions between adjacent cations. This angle is very close to that computed for ThT^+ bound to a model of $A\beta_{1-42}$ fibrils, where π–π and CH–π interactions account for the localization and orientation of ThT^+. These features are fully consistent with anisotropic fluorescence emission studies showing that ThT^+ binds to the fibrils with its long axis parallel to that of fibrils.[21] The computational results give a further insight into this binding at a molecular level and show the relevance of dispersion forces which, as recently reviewed,[24] play a fundamental role in biological sciences. Concerning ThT^+ binding to fibrils, two main stabilizing interactions are present, each involving one of the two moieties: (a) the π–π interaction between the dimethylaniline moiety and the peptide backbone, which can be present regardless of the protein originating the β-sheet structure, and (b) the CH–π interaction between the Gly residue, the only one present in the model peptide, and the benzothiazole moiety. This second interaction, which influences the dihedral angle between the two moieties of ThT^+ and thus its fluorescence properties due to a decrease in torsional relaxation, is dependent on the amino acid residues of the peptide chain. We believe that modulation of this latter interaction by proper molecular design may bring the discovery of new dyes for more specific binding to amyloid fibrils as well as to new diagnostic agents.

We thank the MICINN (CTQ2008-06381/BQU) and DURSI (SGR2009-68 and SGR2009-638) for financial support.

Notes and references

1 H. J. R. Jakob-Roetne and H. Jacobsen, *Angew. Chem., Int. Ed.*, 2009, **48**, 3030–3059.
2 F. Chiti and C. M. Dobson, *Annu. Rev. Biochem.*, 2006, **75**, 333–366.
3 P. S. Vassar and C. F. Culling, *Arch. Pathol.*, 1959, **68**, 487–498.
4 H. LeVine, 3rd, *Protein Sci.*, 1993, **2**, 404–410.
5 V. I. Stsiapura, A. A. Maskevich, V. A. Kuzmitsky, K. K. Turoverov and I. M. Kuznetsova, *J. Phys. Chem. A*, 2007, **111**, 4829–4835.
6 A. Hawe, M. Sutter and W. Jiskoot, *Pharmacol. Res.*, 2008, **25**, 1487–1499.
7 A. Nordberg, *Lancet Neurol.*, 2004, **3**, 519–527.
8 R. Leuma Yona, S. Mazères, P. Faller and E. Gras, *ChemMedChem*, 2008, **3**, 63–66.
9 C. Rodríguez-Rodríguez, N. Sánchez de Groot, A. Rimola, A. Álvarez-Larena, V. Lloveras, J. Vidal-Gancedo, S. Ventura, J. Vendrell, M. Sodupe and P. González-Duarte, *J. Am. Chem. Soc.*, 2009, **131**, 1436–1451.
10 M. Harel, L. K. Sonoda, I. Silman, J. L. Sussman and T. L. Rosenberry, *J. Am. Chem. Soc.*, 2008, **130**, 7856–7861.
11 T. Luhrs, C. Ritter, M. Adrian, D. Riek-Loher, B. Bohrmann, H. Dobeli, D. Schubert and R. Riek, *Proc. Natl. Acad. Sci. U. S. A.*, 2005, **102**, 17342–17347.
12 Crystal data. For **1**: $C_{36}H_{40}Cl_6I_4N_4S_2$, monoclinic, a = 36.297(3), b = 7.1666(5), c = 19.5063(13) Å, β = 112.525(1)°, V = 4687.0(6) $Å^3$, T = 296 K, space group $C2/c$ (no. 15), Z = 4, 15 766 reflections measured, 5775 unique (R_{int} = 0.035) which were used in all calculations, $R(F)$ = 0.052 for 3500 reflections with $I > 2\sigma(I)$, $Rw(F^2)$ = 0.143 for all data. For **2**: $C_{18}H_{20}Cl_3IN_2S$, M = 529.67, monoclinic, a = 7.4500(5), b = 14.7704(9), c = 19.5483(12) Å, β = 94.431(1)°, V = 2144.7(2) $Å^3$, T = 296 K, space group $P2_1/n$ (no. 14), Z = 4, 14 563 reflections measured, 5255 unique (R_{int} = 0.036) which were used in all calculations, $R(F)$ = 0.042 for 3608 reflections with $I > 2\sigma(I)$, $Rw(F^2)$ = 0.096 for all data.
13 C. A. Ilioudis and J. W. Steed, *CrystEngComm*, 2004, **6**, 239–242.
14 D. L. Long, H. M. Hu, J. T. Chen and J. S. Huang, *Acta Crystallogr., Sect. C: Cryst. Struct. Commun.*, 1999, **55**, 339–341.
15 X.-J. Chen, P.-R. Yu, W.-S. Wang and B.-L. Liu, *Acta Crystallogr., Sect. E: Struct. Rep. Online*, 2007, **63**, o595–o596.
16 W.-S. a. G. Wang, Min, Chen, Xiangji, Liu and Boli, *Acta Crystallogr., Sect. E: Struct. Rep. Online*, 2006, **62**, o5668–o5669.
17 Y. Zhang, Z.-H. Su, Q.-Z. Wang and L. Teng, *Acta Crystallogr., Sect. E: Struct. Rep. Online*, 2008, **64**, o2065.
18 C. Lee, W. Yang and R. G. Parr, *Phys. Rev. B: Condens. Matter*, 1988, **37**, 785–789.
19 A. D. Becke, *J. Chem. Phys.*, 1993, **98**, 5648–5652.
20 B. Civalleri, C. M. Zicovich-Wilson, L. Valenzano and P. Ugliengo, *CrystEngComm*, 2008, **10**, 405–410.
21 M. R. Krebs, E. H. Bromley and A. M. Donald, *J. Struct. Biol.*, 2005, **149**, 30–37.
22 C. Wu, Z. Wang, H. Lei, Y. Duan, M. T. Bowers and J. E. Shea, *J. Mol. Biol.*, 2008, **384**, 718–729.
23 J. Aqvist, C. Medina and J. E. Samuelsson, *Protein Eng., Des. Sel.*, 1994, **7**, 385–391.
24 Special Issue—Stacking interactions, *Phys. Chem. Chem. Phys*, ed. P. Hobza, 2008, **10**(19), 2561–2868.

